Electronic Supplementary Material (ESI) for RSC Advances.
This journal is © The Royal Society of Chemistry 2015

Supplementary Information

Decomposition of S-nitroso Species

J. B. Dorado,[a] B. Z. Dlugogorski,[b*] E. M. Kennedy,[a] J. C. Mackie,[a] J. Gore,[c] M. Altarawneh[b]

[a] Process Safety and Environment Protection Research Group, School of Engineering, The University of Newcastle, Callaghan, NSW 2308, Australia

[b] School of Engineering and Information Technology, Murdoch University, 90 South Street, Murdoch WA 6150, Australia. Email: B.Dlugogorski@murdoch.edu.au

[c] Dyno Nobel Asia Pacific Pty. Ltd., Mt Thorley Technical Centre 5 Woodlands Road, Mt. Thorley NSW 2330, Australia

CONTENTS

LIST OF FIGURES

LIST OF TABLES

S1. S-NITROSOTHIOACETAMIDE DECOMPOSITION

Figure S-1 displays first order plots in [RSNO$^+$] where k_{obs} is expected to remain unaffected with varying [RS]. However, linear trendlines depict nonconstant k_{obs} that conveys direct proportionality with [RS] in Fig. S-2. This reaction pathway involving RS possibly arises based on Eq. S1-1. Figure S-1 depicts pseudo first-order plots for which [RS] >> [RSNO$^+$], which allow rate constant calculations from Eq. S1-2. Figure S-2 demonstrates good linearity at high [RS] concentrations where Eq. S1-2 likely predominates. At much lower concentrations of [RS], the contribution of Eq. S1-1 increases in significance and k_{obs} drops.

$$RS + RSNO^+ \rightarrow NO + RSSR^+ \quad \text{(S1-1)}$$

$$k_{obs} = k_2[RS] \quad \text{(S1-2)}$$

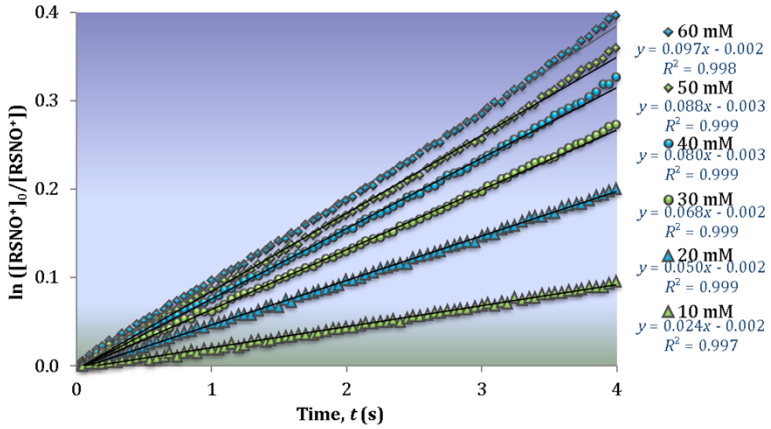

Figure S-1. First order plots $\left(\ln\frac{[A]_0}{[A]} = k_{obs}t\right)$ of S-nitrosothioacetamide decomposition with varying $[RS]_{init}$ while $[NO_2^-]_{init}$ = 2 mM at 1 M $NaClO_4$, pH 1 and 25 °C. In Figs. S-1 through S-5, $[RS]_{init}$ and $[NO_2^-]_{init}$ represent the initial concentrations prior to S-nitrosation. Hence, at the beginning of RSNO$^+$ decay denoted by "0", $[RS]_0 = [RS]_{init} - [RSNO^+]_0$ and similarly for $[NO_2^-]_0$.

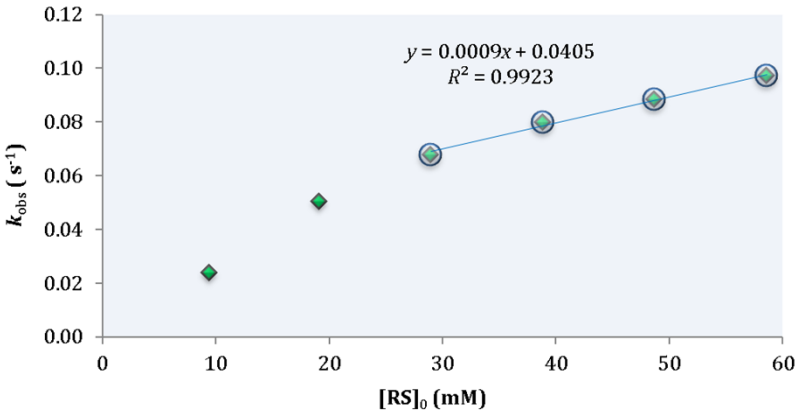

Figure S-2. Linear dependence of k_{obs} obtained from zero-order plots with thioacetamide concentration (in excess), 25 °C. Similar conditions in Fig. S-1.

S1.1. Reaction Mechanism

The chemical system analysed is described by the following reaction mechanism.

$$H^+ + HNO_2 + RS \text{ <==> } RSNO^+ \qquad k_{1f}\ k_{1b}$$
$$RS + RSNO^+ \text{ ----> } NO + RSSR^+ \qquad k_4$$
$$RSNO^+ \text{ <==> } NO + RS^+ \qquad k_{5f}\ k_{5b}$$

The changes in concentrations of chemical species over time are computed by solving and initial value problem described by the following system of differential equations.

$$d[H^+]/dt = -k_{1f}[H^+][HNO_2][RS]+k_{1b}[RSNO^+]$$
$$d[HNO_2]/dt = -k_{1f}[H^+][HNO_2][RS]+k_{1b}[RSNO^+]$$
$$d[RS]/dt = -k_{1f}[H^+][HNO_2][RS]+k_{1b}[RSNO^+]-k_4[RS][RSNO^+]$$
$$d[RSNO^+]/dt = +k_{1f}[H^+][HNO_2][RS]-k_{1b}[RSNO^+]-k_4[RS][RSNO^+]-k_{5f}[RSNO^+]+k_{5b}[NO\cdot][RS^+\cdot]$$
$$d[NO]/dt = +k_4[RS][RSNO^+]+k_{5f}[RSNO^+]-k_{5b}[NO][RS^+]$$
$$d[RSSR^+]/dt = +k_4[RS^+][RSNO^+]$$
$$d[RS^+]/dt = +k_{5f}[RSNO^+]-k_{5b}[NO][RS^+]$$

S1.2. Arrhenius and Data–Model Concentration–Time Plots

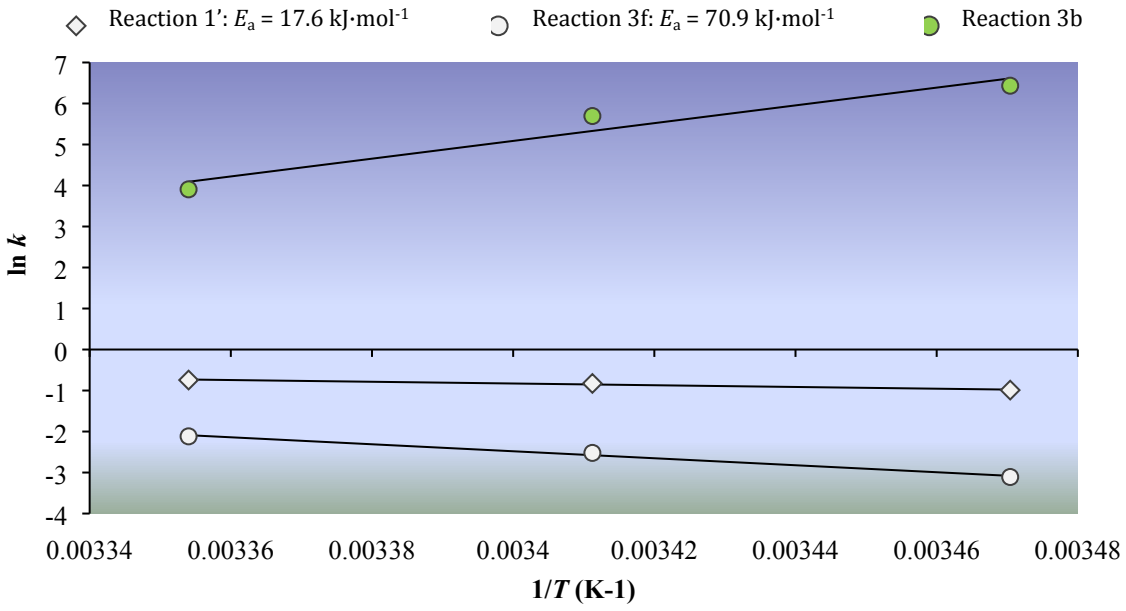

Figure S-3. Arrhenius plots for determination of activation energy for S-nitrosothiacetamide decomposition.

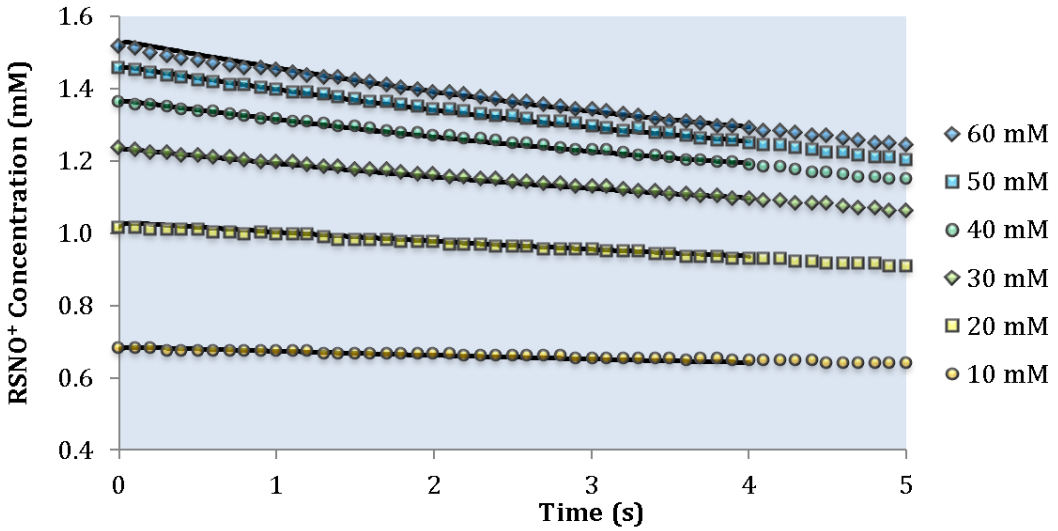

Figure S-4. Overlap of experimental data and kinetic model for S-nitrosothiacetamide decomposition, for varying $[RS]_{init}$. $[H^+]$ = 0.1 M, $[NO_2^-]_{init}$ = 0.002 M, I = 1 M, $NaClO_4$ and 15 °C.

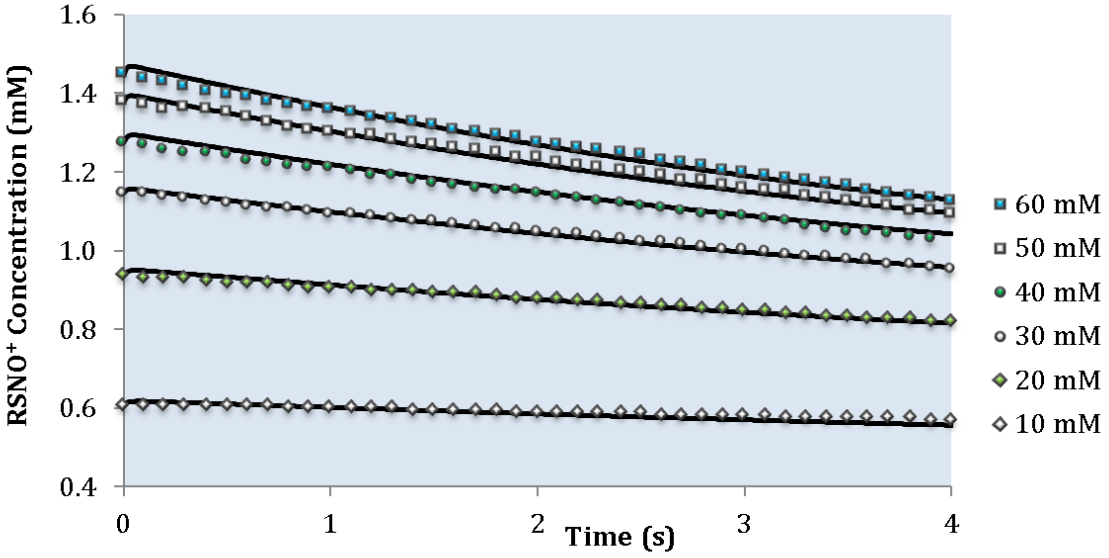

Figure S-5. Overlap of experimental data and kinetic model for S-nitrosothiacetamide decomposition, for varying $[RS]_{init}$. $[H^+]$ = 0.1 M, $[NO_2^-]_{init}$ = 0.002 M, I = 1 M, $NaClO_4$ and 20 °C.

S2. RATE CONSTANTS: S-NITROSATION AND HNO_2 DECOMPOSITION

Table S-1: Kinetic rate constants for S-nitrosation of thioacetamide and thiourea and for HNO_2 decomposition

Reaction			Temperature (°C)						
			15	20	25	30	35	40	45
S-nitrosation									
$H + HNO_2 + RS \rightleftharpoons RSNO^+$	(RS = Thioacetamide)	k_f, $M^{-2}\cdot s^{-1}$	7 310	11 500	15 800				
		k_b, s^{-1}	12.6	23.5	40				
	(RS = Thiourea)	k_f, $M^{-2}\cdot s^{-1}$	9 490	15 300	24 000	37 200	48 300	72 000	91 300
		k_b, s^{-1}	0.8	1.8	2.9	5.6	9.3	15.1	24.3
HNO_2 *Decomposition*									
$HNO_2 + HNO_2 \rightleftharpoons NO\cdot + NO_2$		k_f	1.59	3.01	5.60	10.2	18.2	31.9	54.9
		k_b	1.61×10^{7}	2.21×10^{7}	3.00×10^{7}	4.03×10^{7}	5.36×10^{7}	7.08×10^{7}	9.25×10^{7}
		K_t	9.86×10^{-8}	1.36×10^{-7}	1.87×10^{-7}	2.53×10^{-7}	3.39×10^{-7}	4.51×10^{-7}	5.93×10^{-7}
	Activation energy	E_a, $kJ\cdot mol^{-1}$	90						
	Enthalpy change of reaction	ΔH^{θ}, kJ	45.6						
$NO_2 + NO_2 \rightleftharpoons HNO_2 + NO_3$		k_f	5.52×10^{7}	6.23×10^{7}	7.00×10^{7}	1.27×10^{8}	8.74×10^{8}	9.72×10^{8}	1.08×10^{9}
		k_b	1.97×10^{-3}	4.24×10^{-3}	8.90×10^{-3}	2.96×10^{-2}	3.65×10^{-2}	7.13×10^{-2}	1.37×10^{-1}
		K_t	2.80×10^{10}	1.47×10^{10}	7.87×10^{9}	4.30×10^{9}	2.40×10^{9}	1.36×10^{9}	7.88×10^{8}
	Activation energy	E_a, $kJ\cdot mol^{-1}$	17						
	Enthalpy change of reaction	ΔH^{θ}, kJ	-90.7						

S3. FORMATION OF SULFUR

Figure S-6 illustrates a small peak that precedes the rapid rise in absorbance due to sulfur precipitates in S-nitrosothioacetamide decomposition. The induction period is dependent on the temperature (Fig. S-7) but not significantly on initial S-nitrosothioacetamide concentration (Fig S-8). This implies that the rate limiting reaction for S_8 precipitation is not the initial decomposition but a subsequent reaction from decomposition products.

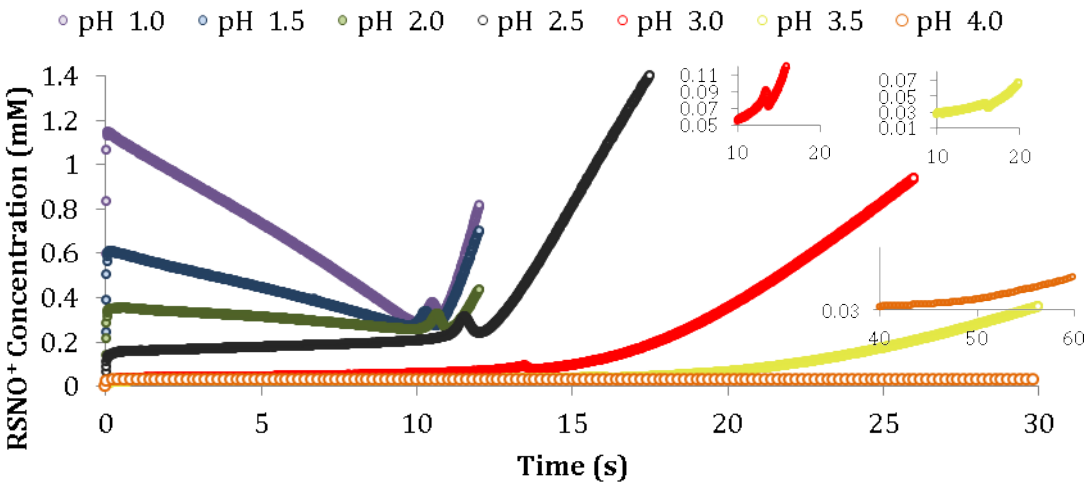

Figure S-6. $RSNO^+$ concentration of S-nitrosothioacetamide at pH 1–4 and 25 °C with $[NO_2^-]_{init}$ = 2 mM, $[CH_3NH_2CS]$ = 40 mM, I = 1 M, $NaClO_4$, 420 nm.

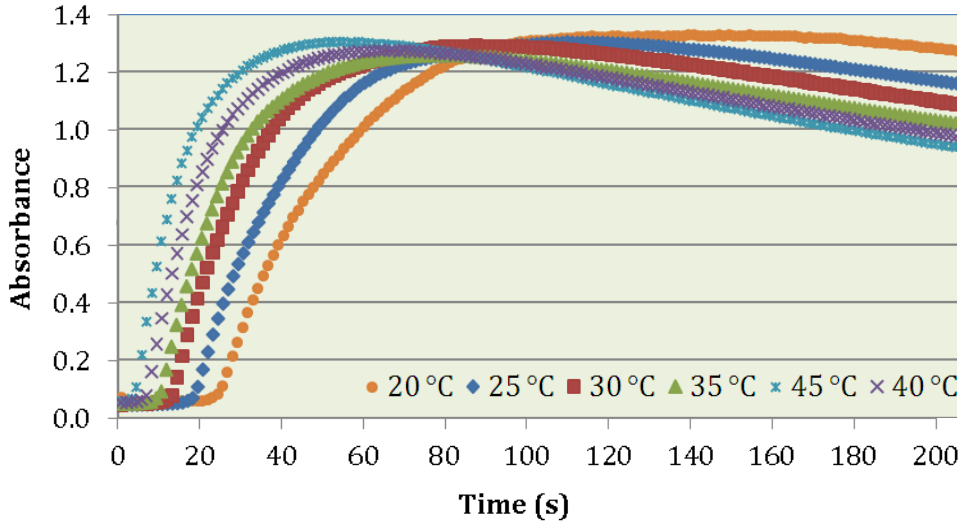

Figure S-7. Absorbance plot of S-nitrosothioacetamide formation at varying temperature and with 1 mM $NaNO_2$, thioacetamide in excess (10$[NO_2^-]$).

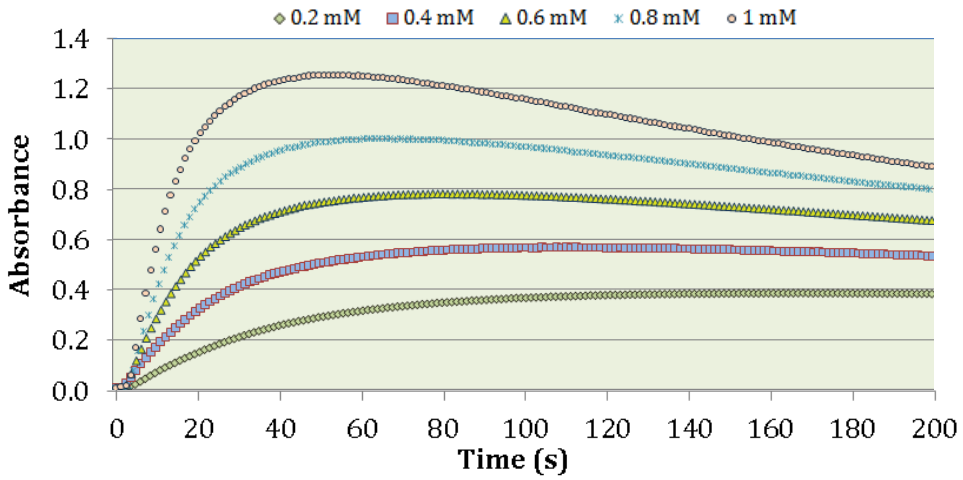

Figure S-8. Typical absorbance plot of S-nitrosothioacetamide formation with varying nitrite at 45 °C for 0.5 M $NaClO_4$, 0.04 M $HClO_4$ and thioacetamide in excess (10[NO_2^-]), collected at 420 nm.

Garcia and Druschel observed that nanoparticle formation from single S^0 molecules to S_8 occurs in seconds followed by subsequent coarsening into micron-sized particles (Ostwald ripening and aggregation) that is strongly temperature dependent and partly pH dependent with coarsening proceeding faster at pH 3 compared to pH 7 or 10.[1] In precipitating systems, two important size enlargement mechanisms are aggregation and growth. Aggregation refers to the process in which a particle collides with another particle and forms a bigger particle, while growth pertains to deposition of a non-particulate material on the surface of a particle. Using particle size distribution (PSD) by analysis of precipitation suspension, Bramley et al. found that the growth rate is second order in a relative supersaturation regardless of reactant composition while aggregation rate exhibits a more complex dependence on solution composition.[2] In another work, Bramley et al. developed a methodology for extracting aggregation and growth rates from experimental data (i.e., from PSDs).[3] Thus, these two peaks are attributed to the colloidal phase of solution during decomposition, which forms S_8 as a product.

An earlier book by Weiser in 1933 further lends possible explanation to signals observed.[4] The first small peak represents the rapid transition as the particle size increases by coagulation. Sulfur colloidal solutions exhibit a wide variation in color with change in particle size — the original blue solution of sulfur in pyrosulfuric acid, upon dilution of sulfuric acid which lowers the solubility of sulfur, changes consecutively to green, yellow, orange, red,

violet and to a second cloudy blue to green.[4] Moreover, the absorbance A_λ of a solution as a function of wavelength when the solution is composed of non-absorbing colloidal particles is expressed as Eq. S3-1, where l is the cell path length and C_{sca} denotes the cross section for scattering represented by Eq. S3-2 for a mono-dispersion colloidal system.

$$A_\lambda = \log e \cdot C_{sca} \cdot l \tag{S3-1}$$

$$C_{sca} = \pi r^2 N Q_{sca} \tag{S3-2}$$

In the last equation, r denotes the radius of each mono-dispersed particle, N depicts the number of particles per unit volume, and Q_{sca} represents the scattering efficiency.[5] At a single wavelength, 420 nm in this case, the small and narrow peak observed just before the opalescence shows an increase in absorbance possibly from increase in particle radius and the sudden drop possibly as the number of particles drop from aggregation into bigger particles which then paved way for the second peak observed. The second larger peak arises due to the weak opalescence (indicating presence of colloid particles) formed as the solution changes to yellow until S_8 precipitates out. In Fig. S-9, the very broad peak observed during experiments coincides with the spectral absorbance of colloidal sulfur reported by Samukawa et al.[5] The particles in the milky white solution measures up to 0.8 μm in diameter. Due to low solubility of S_8 in water of ~1×10^{-4} mM, these eventually precipitate and form crystal aggregates up to 50 μm diameter.[6]

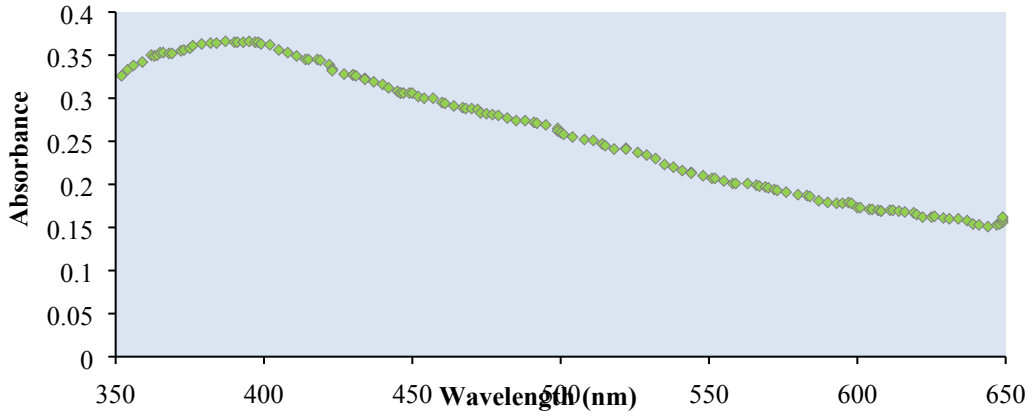

Figure S-9. Spectral absorbance of colloidal sulfur solution.[5]

S4. DECOMPOSITION KINETICS: S-NITROSOTHIOUREA

S4.1. Reaction Mechanism 1

The chemical system analyzed is described by the following reaction mechanism.

$$\begin{aligned} RSNO^+ + RS &\text{ <==> } NO + RSSR^+ && k_{1f}\ k_{1b} \\ RSNO^+ + RSNO^+ &\text{ ----> } NO + NO + RSSR^{2+} && k_2 \end{aligned}$$

The changes in concentrations of chemical species over time are computed by solving and initial value problem described by the following system of differential equations.

$$\begin{aligned} d[RSNO^+]/dt &= -k_{1f}[RSNO^+][RS]+k_{1b}[NO][RSSR^+]-k_2[RSNO^+][RSNO^+]-k_2[RSNO^+][RSNO^+] \\ d[RS]/dt &= -k_{1f}[RSNO^+][RS]+k_{1b}[NO][RSSR^+] \\ d[NO]/dt &= +k_{1f}[RSNO^+][RS]-k_{1b}[NO][RSSR^+]+k_2[RSNO^+][RSNO^+]+k_2[RSNO^+][RSNO^+] \\ d[RSSR^+]/dt &= +k_{1f}[RSNO^+][RS]-k_{1b}[NO][RSSR^+] \\ d[RSSR^{2+}]/dt &= +k_2[RSNO^+][RSNO^+] \end{aligned}$$

S4.2. Reaction Mechanism 2

The chemical system analyzed is described by the following reaction mechanism:

$$\begin{aligned} H^+ + HNO_2 + RS &\text{ <==> } RSNO^+ && k_{0f}\ k_{0b} \\ RS + RSNO^+ &\text{ <==> } NO + RSSR^+ && k_{1f}\ k_{1b} \\ RSNO^+ &\text{ <==> } NO + RS^+ && k_{2f}\ k_{2b} \\ RSNO^+ + RSNO^+ &\text{ ----> } NO + NO + RSSR^{2+} && k_3 \end{aligned}$$

The changes in concentrations of chemical species over time are computed by solving an initial value problem described by the following system of ordinary differential equations:

$$\begin{aligned} d[H^+]/dt &= -k_{0f}[H^+][HNO_2][RS]+k_{0b}[RSNO^+] \\ d[HNO_2]/dt &= -k_{0f}[H^+][HNO_2][RS]+k_{0b}[RSNO^+] \\ d[RS]/dt &= -k_{0f}[H^+][HNO_2][RS]+k_{0b}[RSNO^+]-k_{1f}[RS][RSNO^+]+k_{1b}[NO][RSSR^+] \\ d[RSNO^+]/dt &= +k_{0f}[H^+][HNO_2][RS]-k_{0b}[RSNO^+]-k_{1f}[RS][RSNO^+]+k_{1b}[NO][RSSR^+]- \\ &\quad k_{2f}[RSNO]+k_{2b}[NO][RS^+]-k_3[RSNO^+][RSNO^+]-k_3[RSNO^+][RSNO^+] \\ d[NO]/dt &= +k_{1f}[RS][RSNO^+]-k_{1b}[NO][RSSR^+]+k_{2f}[RSNO^+]-k_{2b}[NO][RS^+]+k_3[RSNO^+][\end{aligned}$$

$$\begin{aligned} & \mathrm{RSNO^+}]+k_3[\mathrm{RSNO^+}][\ \mathrm{RSNO^+}] \\ \mathrm{d}\ [\mathrm{RSSR^+}]/\mathrm{d}t = & +k_{1\mathrm{f}}[\mathrm{RS}][\ \mathrm{RSNO^+}]-k_{1\mathrm{b}}[\mathrm{NO}][\ \mathrm{RSSR^+}] \\ \mathrm{d}\ [\mathrm{RS^+}]/\mathrm{d}t = & +k_{2\mathrm{f}}[\mathrm{RSNO^+}]-k_{2\mathrm{b}}[\mathrm{NO}][\ \mathrm{RS^+}] \\ \mathrm{d}\ [\mathrm{RSSR^{2+}}]/\mathrm{d}t = & +k_3[\mathrm{RSNO^+}][\ \mathrm{RSNO^+}] \end{aligned}$$

S5. EFFECT OF EDTA ADDITION

We studied the effect of EDTA addition (chelating agent for Cu ions that may be adventitiously present) on nitrosation. Figure S-10 shows typical absorbance plots at 420 nm for S-nitrothiourea formation, with no apparent effect on the decomposition kinetics (based on Table S-2) — thus, obviating the need for EDTA addition.

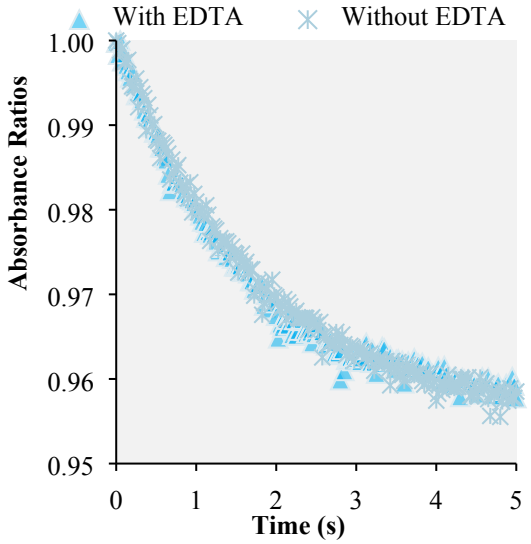

Figure S-10. Absorbance ratio plots of S-nitroso adduct formation with and without 0.25 mM EDTA at 2 mM nitrite, 20 mM thiourea and 0.2 M $HClO_4$, 25 °C at 420 nm.

Table S-2: Maximum absorbance and standard deviation for plot in Fig. S-10 (n = 5).

	With EDTA	Without EDTA	$A_{EDTA}/A_{NO\text{-}EDTA}$ (%)
Mean	**0.2075**	**0.2113**	**98.2**
Standard deviation, %*A*	**0.45**	**0.53**	

S6. THIOUREA AND THIOACETAMIDE NITROSATION, PH 2

Figures S-11 and S-12 show nitrosation reaction at a pH of 2 (0.1 M H_3PO_4 + 0.1 M KH_2PO_4), I = 1 M $NaClO_4$ and 25 °C with $[TA]_{init}$ or $[TU]_{init}$ = 0.040 M and $[NO_2^{-1}]_{init}$ = 0.002 M in anaerobic conditions. These are raw aborbance plots during wide wavelength scans, where detection is not fast enough to capture initial $RSNO^+$ absorbance; hence, nonzero intercepts at t =0.

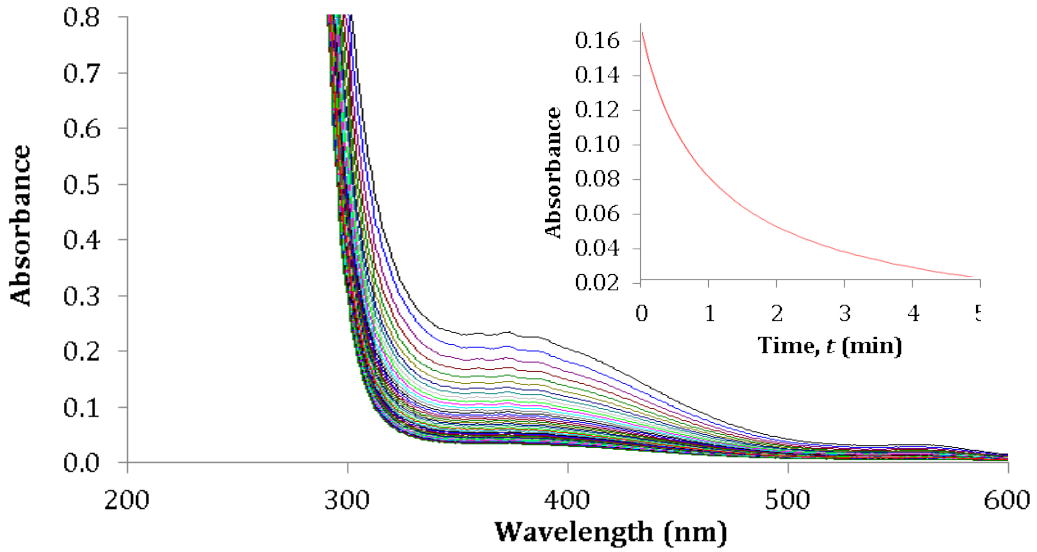

Figure S-11. UV-vis spectra and decay curve at 420 nm for thiourea nitrosation, pH 2 and 25°C.

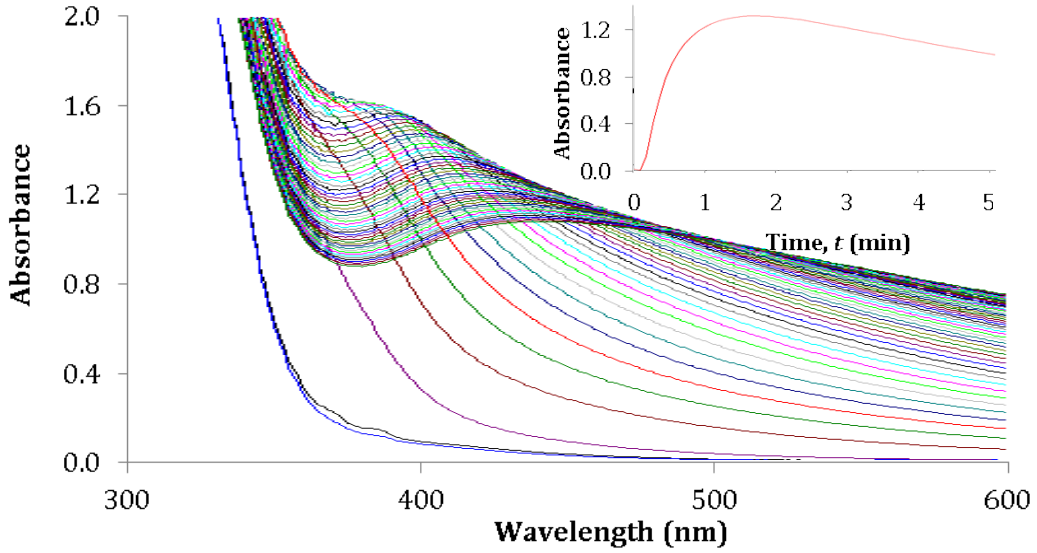

Figure S-12. UV-vis spectra and decay curve at 420 nm for thioacetamide nitrosation, pH 2 and 25°C.

From the kinetics continuum, the reactions were found to have reached equilibrium in less than 200 and 500 ms, for thioacetamide and thiourea, respectively. At these time regimes, the parallel decomposition pathways of the substrates in acidic media should not impact the kinetics significantly (i.e., << 0.04[Substrate]).

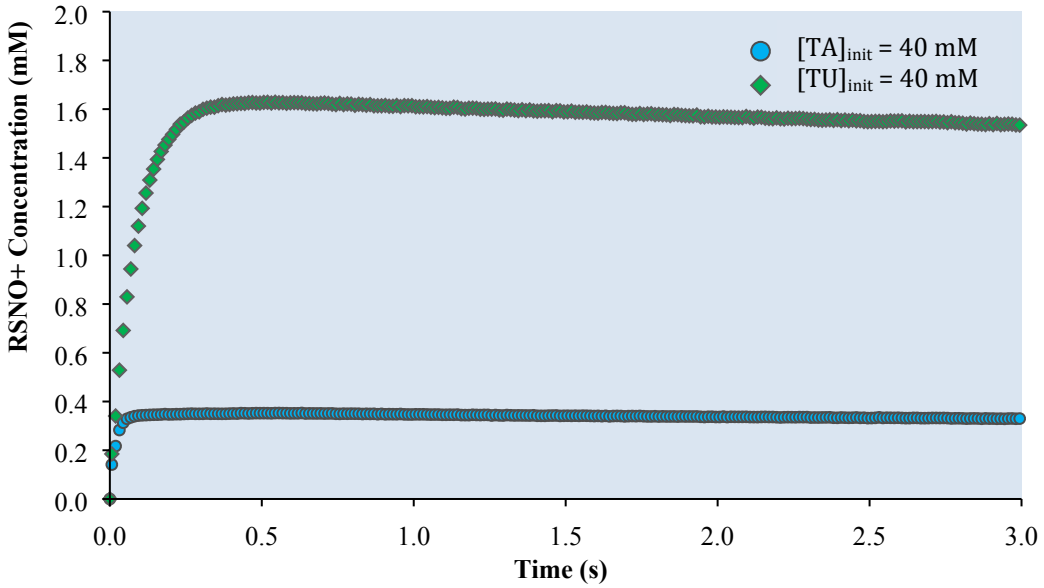

Figure S-13. $RSNO^+$ concentration from kinetics continuum at 420 nm, 12.5 ms sampling interval for thioacetamide and thiourea nitrosation, pH 2 and 25 °C. Equilibrium concentration at 1.62 ± 0.01 mM (n = 18) and 0.351 ± 0.005 (n = 27) for thiourea and thioacetamide, respectively, at $[NO_2^-]_{init}$ = 2 mM.

S7. FURTHER COMMENTS TO SECTION GAS-PHASE DETECTION OF PRODUCTS

NO test for NH_3 formation was carried out for this paper, to verify interference in detection for NO_x chemiluminescence. In context of TU decomposition, this pathway was found to be too slow to be considered important (in a separate study involving extended discussion on NH_3 detection). Urea, known to decompose to NH_4^+ ions, tested positive in litmus paper upon addition of sodium hydroxide. Gas-phase FTIR spectroscopy did not detect NH_3 at all, and our test results suggest that Nafion dryer strips the sample stream of NH_3. As such, even if there are minute NH_3 concentrations produced in a parallel substrate decomposition, it is unlikely to affect significantly on NO_x quantification.

S8. THEORETICAL CALCULATIONS

The reaction enthalpies obtained using different solvation models for decomposition mechanisms are outlined in the following tables.

Table S-3: Theoretical calculations for enthalpies of reaction of S-nitrosothioacetamide decomposition

REACTION	ΔH^{θ}, kJ				
	SM 1	SM2	SM3	SM4	SM5
RS + H + HNO_2 = RSNO + H_2O	28.5	32.7	24.3	8.3	26.1
$RSNO^+$ + RS = $RSSR^+$ + NO	104	95.1	94.5	95.1	99.4
$RSNO^+$ = RS^+ + NO	28.5	32.7	24.3	8.3	26.1

SM1: IEFPCM/UFF, UB3LYP/6-311G(d,p)
SM2: B3LYP/6-311+G(d,p) CPCM (UAHF)
SM3: B3LYP/6-311+G(d,p) CPCM (UAHF)
SM4: M052X/6-311+G(d,p) SMD
SM5: B3LYP/6-311+G(d,p) SMD

Table S-4: Reaction mechanism for S-nitrosothiourea decomposition (Mechanism 3)

REACTION	ΔH^{θ}, kJ			
	SM 1	SM2	SM3	SM4
Mechanism 1: Literature				
$RSNO^+$ + RS = $RSSR^+$ + NO	31.7	38.5	8.7	31.3
$RSNO^+$ + $RSNO^+$ = $RSSR^{2+}$ + 2NO	32.6	20.1	-22.5	25.4
Mechanism 3				
$RSNO^+$ + RS = $RSSR^+$ + NO	31.7	38.5	8.7	31.3
RSNO = RS^+ + NO	112.8	111.1	96.7	108.2
$RSNO^+$ + $RSNO^+$ = $RSSR^{2+}$ + 2NO	32.6	20.1	-22.5	25.4

SM1: IEFPCM/UFF, UB3LYP/6-311G(d,p)
SM2: B3LYP/6-311+G(d,p) CPCM (UAHF)
SM3: M052X/6-311+G(d,p) SMD
SM4: B3LYP/6-311+G(d,p) SMD

S9. MISCELLANEOUS FIGURES

The figures below show Arrhenius plots for the reaction mechanisms discussed in main text.

Table S-5: Reactions involved in S-nitrosothiourea decomposition

EQUATION NO.	REACTION
1’	$RSNO^+ = RS^{+}\cdot + NO\cdot$
3	$RSNO^+ + RS = RSSR^{+}\cdot + NO\cdot$
4	$RSNO^+ + RSNO^+ = RSSR^{2+} + 2NO\cdot$

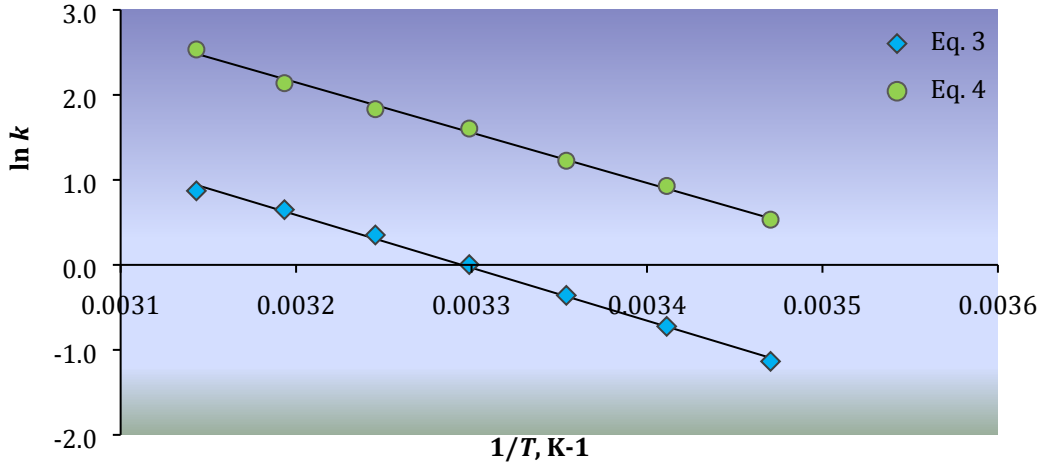

Figure S-14. Arrhenius plots for S-nitrosothiourea decomposition, Mechanism 2: Eqs. 3 and 4, 25–45 °C.

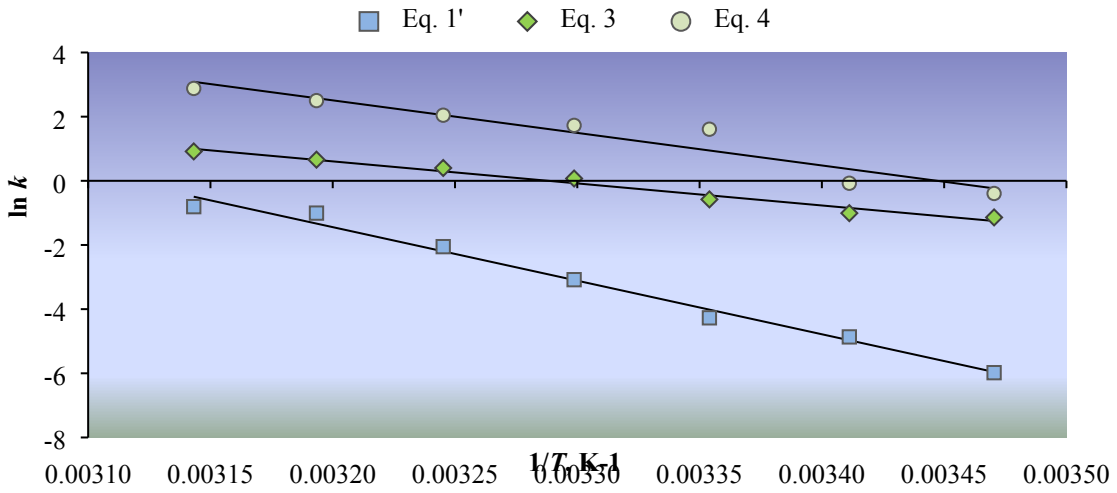

Figure S-15. Arrhenius plots for decomposition of S-nitrosothiourea, Mechanism 3: Eqs. 1’, 3, and 4. Experiment conditions: $[H^+]$ = 0.1 M $HClO_4$, I = 1 M, $NaClO_4$.

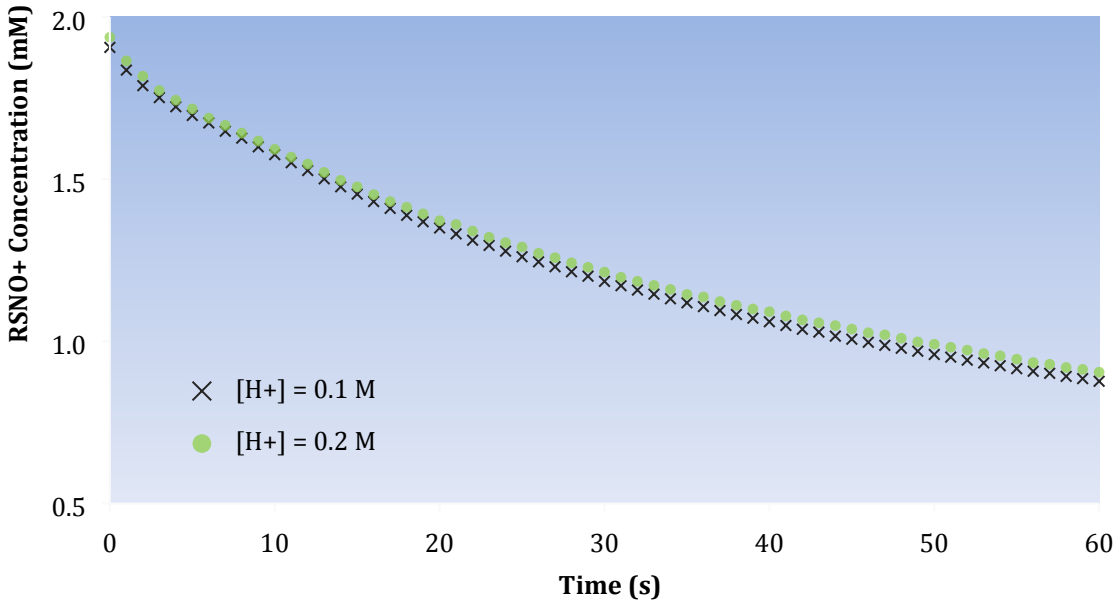

Figure S-16. Effect of acidity on decomposition of S-nitrosothiourea at 25 °C. Experiment conditions are $[NO_2^-]_{init}$ = 0.002 M, $[RS]_{init}$ = 0.04 M and I = 1 M, $NaClO_4$.

S10. REFERENCES

(1) Garcia, A. E.; Druschel, G. *Mineralogical Magazine* **2012**, *76*.
(2) Bramley, A. S.; Hounslow, M. J.; Newman, R.; Paterson, W. R.; Pogessi, C. *Chemical Engineering Research and Design* **1997**, *75*, 119.
(3) Bramley, A. S.; Hounslow, M. J.; Ryall, R. L. *Journal of Colloid and Interface Science* **1996**, *183*, 155.
(4) Weiser, H. B. In *Inorganic Colloid Chemistry* J. Wiley & Sons; Chapman & Hall: New York; London, 1933; Vol. 1.
(5) Samukawa, T.; Onitsuka, M.; Ohta, K.; Tominaga, M.; Yoshiyama, H. *J Oceanogr* **1992**, *48*, 129.
(6) Steudel, R. In *Elemental Sulfur and Sulfur-Rich Compounds I*; Steudel, R., Ed.; Springer Berlin Heidelberg: 2003; Vol. 230, p 153.